Dynamic Safety Assessment of a Nonlinear Pumped-Storage Generating System in a Transient Process

Huanhuan Li[1,2], Diyi Chen[1,2*], Ehsan Arzaghi[3], Rouzbeh Abbassi[3,7], Adem Kilicman[4], Tomas Caraballo[5], Edoardo Patelli[6], Xiang Gao[1,2], Beibei Xu[1,2]

[1]Institute of Water Resources and Hydropower Research, Northwest A&F University, Shaanxi Yangling 712100, P. R. China
[2]Key Laboratory of Agricultural Soil and Water Engineering in Arid and Semiarid Areas, Ministry of Education, Northwest A&F University, Shaanxi Yangling 712100, P. R. China
[3]National Centre of Maritime Engineering and Hydrodynamics, Australian Maritime College (AMC), University of Tasmania, Launceston, Tas, Australia
[4]Department of Mathematics, University Putra Malaysia, 43400 UPM, Serdang, Selangor, Malaysia
[5]Department of Ecuaciones Diferenciales & Analysis Numerical, University of Sevilla, Apdo Correos 1160, E-41080 Seville, Spain
[6]Institute for Risk and Uncertainty, University of Liverpool, Peach Street, Chadwick Building, Liverpool L69 7ZF, United Kingdom
[7]School of Engineering, Faculty of Science and Engineering, Macquarie University, Sydney, NSW, Australia

Corresponding author: Diyi Chen
Mailing Address: Institute of Water Resources and Hydropower Research, Northwest A&F University, Shaanxi Yangling 712100, China
Telephones: 086-181-6198-0277
E-mail: diyichen@nwsuaf.edu.cn

Abstract: This paper focuses on a pumped-storage generating system with a reversible Francis turbine and presents an innovative framework for safety assessment in an attempt to overcome their limitations. Thus the aim is to analyze the dynamic safety process and risk probability of the above nonlinear generating system. This study is carried out based on an existing pumped-storage power station. In this paper we show the dynamic safety evaluation process and risk probability of the nonlinear generating system using Fisher discriminant method. A comparison analysis for the safety assessment is performed between two different closing laws, namely the separate mode only to include a guide vane and the linkage mode that includes a guide vane and a ball valve. We find that the most unfavorable condition of the generating system occurs in the final stage of the load rejection transient process. It is also demonstrated that there is no risk to the generating system with the linkage mode but the risk probability of the separate mode is 6 percent. The results obtained are in good agreement with the actual operation of hydropower stations. The developed framework may not only be adopted for the applications of the pumped-storage generating system with a reversible Francis turbine but serves as the basis for the safety assessment of various engineering applications.

Keywords: Pumped-storage generating system; Francis turbine; dynamic safety analysis; risk probability; transient process

1. Introduction

Pumped-storage generating system with a reversible Francis turbine (PSGS) performs as a nonlinear multi-purpose engineering equipment for power production and power consumption, enhancing the efficiency and reliability of electrical power systems [1-2]. Today, the average estimated growth rate of PSGS increases 10% annually in the world, with a total installed capacity of more than 100 GW [3-6]. Pumped-storage power stations are built to improve the maximum usage of thermal and nuclear power as well as to guarantee a high quality of power supply [7].

PSGSs are complex nonlinear systems incorporating a great deal of uncertainty in the operation of their hydraulic, mechanical and electrical components [8-11]. Based on five fundamental conditions (i.e., static, generating and pumping condition as well as generating/pumping transfer to phase modulation), PSGSs provide twenty-four switching modes such as start-up in pumping/generating condition switch to shut-down, start-up in pumping/generating condition switch to load rejection, and static switch to pumping condition due to the different demands of the electricity generation in hydropower stations [12-14]. This results in a substantial level of safety challenges such as vibration and water hammer pressure amplitudes in the penstock and draft tube [15-19]. From the operational principle of PSGSs, the above-mentioned safety challenges highlight the need for analyzing the S and inverted-S domains for the operation of pump mode, turbine mode, braking mode in the pumping/generating condition and reversed pump mode. For example, due to the decrease of the pump-turbine flow during the load rejection transient, the generating system can enter the reversed pump mode meaning that the pump-turbine runs in reverse [20]. This in turn causes a higher pump-turbine speed with respect to three different values of the pump-turbine flow. It is therefore considered a hazard, thus, requiring more attention in safety assessment of PSGSs.

Over recent decades, safety assessment methods have been developed in many fields including information science and bioscience. In the case of engineering applications some of these methods can quantitatively describe the uncertainty of the phenomena and provide failure probability of systems or their components [21-23]. In the literatures [24-25], two main approaches are considered for safety assessment, namely static and dynamic processes. The static assessment approach is used to predict the safety property of the system at a certain time, and it cannot better reveal the dynamic behaviors varying with real time. Meanwhile, the static assessment approach may ignore some fuzzy information in the system due to the simple algorithm design. Conversely, the dynamic assessment approach has the ability to quantify dynamic risks in transient processes by updating the information of the critical factors of the system in real time. The static assessment has been widely investigated by previous researchers, while the application of the dynamic approach is relatively limited, mainly due to complexity of the method. Currently, there are copious research outcomes available on PSGSs mainly focusing on dimensional design, hydrological computation, transient simulation and fault diagnosis aspects. However, not many investigations aim at assessing the safety of these systems. Safety assessment of PSGSs aims to predict the failure probability of the system in static and/or dynamic processes enabling the improvement of operation reliability. This requires developing a sound methodology and evaluative standard for an advanced safety assessment, given the complexity of PSGS.

This paper aims at developing a methodology which assesses the dynamic safety of PSGS operations. The novelty of this research is attributed to three components that include: a) proposing a dynamic safety assessment framework for PSGSs, b) conducting the dynamic safety evaluation process and quantification of risk probability values for the nonlinear generating system under different engineered closing laws, i.e. the separate mode operating with a guide vane and the linkage mode operating with a guide vane and a ball valve, and c) utilizing the Fisher discriminant analysis (FDA) method on the basis of actual operating data for the analyses.

Table 1: Nomenclature of the pumped-storage generating system with a reversible Francis turbine

Symbol	Quantity
H_l	the piezometric head of penstock, m
α	the angle between penstock and horizontal direction, rad
D	the diameter of penstock, m
a	the water hammer wave speed, m/s
f	the Darcy-westbach resistance coefficient
g	the gravitational acceleration, m/s^2
v	the flow velocity, m/s
x	the displacement along penstock direction, m
q_1	the deviation of the pump-turbine flow, p.u.
q_2	the deviation of the tailrace pipe flow, p.u.
z_s	the deviation of the water level of surge tank, p.u.
n	the deviation of the pump-turbine speed, p.u.
u_{ij}	an intermediate variable
Q	the pump-turbine flow at arbitrary working point, m^3/s
Q_{11}	the unit pump-turbine flow, m^3/s
N	the pump-turbine speed at arbitrary working point, rad/s
N_{11}	the unit pump-turbine speed, rad/s
D_1	the inlet diameter of runner, m
H	the pump-turbine head, m
M_t	the pump-turbine torque at arbitrary working point, N·m
T_a	the inertial time constant of generator rotor, s
α_1	the coefficient of friction resistance of penstock
T_{w1}	the water starting time of penstock, s
K_1, K_2	an intermediate variables
F	the area of surge tank, m^2
T_{w2}	the water starting time of tailrace pipe, s
α_2	the coefficient of friction resistance of tailrace pipe

2. Pumped-storage generating system with a reversible Francis turbine

A pumped-storage generating system with a reversible Francis turbine (PSGS) that incorporates hydraulic, mechanical and electrical components is the complex dual-use equipment as it undertakes the critical tasks of generating power in peak-load hours and pumping in low-load hours. A schematic of

PSGS working mechanism is illustrated in Fig. 1.

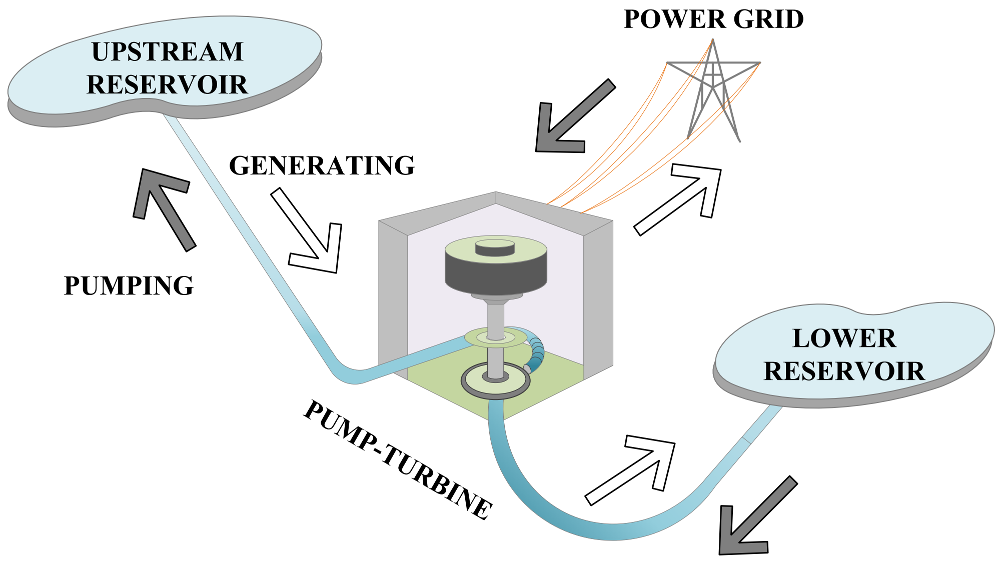

Fig. 1. Schematic working mechanism of an PSGS.

2.1 PSGS Model

The basic dynamic behavior of an PSGS is expressed by the motion equation and continuity equation shown in Eq. (1) and (2). Using the method of characteristics performed in literatures [26-28], we further convert the Eq. (1) and (2) into the equations of characteristic lines. Additionally, the detailed boundary conditions of the studied PSGS model can also be found in references [26-28].

$$\text{Motion equation of flow}: g\frac{\partial H_1}{\partial x}+\frac{\partial v}{\partial t}+v\frac{\partial v}{\partial x}+\frac{fv|v|}{2D}=0, \tag{1}$$

$$\text{Continuity equation of flow}: \frac{\partial H_1}{\partial t}+v\frac{\partial H_1}{\partial x}+\frac{a^2}{g}\frac{\partial v}{\partial x}+v\sin\alpha=0, \tag{2}$$

where H_1, α, D, a, f, g, v and x are the piezometric head of penstock, the angle between penstock and horizontal direction, the diameter of penstock, the water hammer wave speed, Darcy-westbach resistance coefficient, the gravitational acceleration, the flow velocity and the displacement along penstock direction, respectively.

In this work, we focus on the transient safety analysis of the PSGS, thus a validated PSGS model presented in literatures [26-28] is introduced using the method of characteristics. Correspondingly, the validated PSGS model can be expressed as Eq. (3), and the detailed deducing steps are performed in the references [26-28].

$$\begin{bmatrix} \frac{dq_1}{dt} \\ \frac{dq_2}{dt} \\ \frac{dz_s}{dt} \\ \frac{dn}{dt} \end{bmatrix} = \begin{bmatrix} u_{11} & 0 & u_{13} & u_{14} \\ 0 & u_{22} & u_{23} & 0 \\ u_{31} & u_{32} & 0 & 0 \\ u_{41} & 0 & 0 & u_{44} \end{bmatrix} \begin{bmatrix} q_1 \\ q_2 \\ z_s \\ n \end{bmatrix}, \tag{3}$$

where q_1, q_2, z_s and n are the deviations of the pump-turbine flow, the tailrace pipe flow, the water level of surge tank and the pump-turbine speed; u_{ij} (i = 1, 2, …, 4 and j = 1, 2, …, 4) denotes an intermediate variable, and it can be described as:

$$\begin{cases} u_{11} = -\frac{K_1 |Q| \sqrt{H}}{T_{w1}} - \frac{2\sqrt{H}}{(Q - \frac{dQ}{dN} N) T_{w1}} \\ u_{13} = -\frac{1}{T_{w1}} \\ u_{14} = \frac{2\sqrt{H} \frac{dQ}{dN}}{T_{w1} (Q - N \frac{dQ}{dN})} \end{cases}, \tag{4}$$

$$\begin{cases} u_{22} = -\frac{K_2 |Q| \sqrt{H}}{T_{w2}} \\ u_{23} = \frac{1}{T_{w2}} \end{cases}, \tag{5}$$

$$\begin{cases} u_{31} = \dfrac{Q}{HF} \\ u_{32} = -\dfrac{Q}{HF} \end{cases} \tag{6}$$

and

$$\begin{cases} u_{41} = \sqrt{H}\dfrac{2M_t - N\dfrac{dM_t}{dN}}{T_a(Q - N\dfrac{dQ}{dN})} \\ u_{44} = \dfrac{\sqrt{H}}{T_a}\dfrac{Q\dfrac{dM_t}{dN} - 2M_t\dfrac{dQ}{dN}}{Q - N\dfrac{dQ}{dN}} \end{cases}, \tag{7}$$

where Q, N, H and M_t are the pump-turbine flow, the pump-turbine speed, the pump-turbine head and the pump-turbine torque at arbitrary working point, respectively; T_{w1}, T_{w2}, F and T_a are the water starting time of penstock, the water starting time of tailrace pipe, the area of surge tank and the inertial time constant of generator rotor, respectively; K_1 and K_2 are the intermediate variables, $K_1=2\alpha_1 D_1^4 Q_{11}^2$ and $K_2=2\alpha_2 D_1^4 Q_{11}^2$. α_1, α_2, D_1 and Q_{11} are the coefficient of friction resistance of tailrace pipe, the coefficient of friction resistance of penstock, the inlet diameter of runner and the unit pump-turbine flow, respectively.

2.2 100% Load Rejection Transient Process of PSGS

A nonlinear PSGS can at least operate in twenty-four switching modes [12-14] during which transient processes such as the loss of pump-power, the load rejection and pump shutdown may occur. The present paper aims at assessing the 100% load rejection which is a common high-risk accident in the generating mode of PSGS operation. The 100% load rejection is considered as a significant hazard for the PSGSs, inducing adverse changes to the monitored system parameters. PSGS runs in inverted-S domain during this load rejection transient leading to an undesired situation where the generating system is operating with only one pump-turbine speed with respect to three different values of the pump-turbine flow. Here, as mentioned in the references. [1, 20], the inverted-S domain refers to the PSGS operates from the turbine mode to the reversed pump mode. The pump-turbine speed plays a critical role in the stability of PSGS as it directly influences the changes in the flow and water-hammer pressure in the penstock.

Based on the above discussion, different closing laws of the closing devices are therefore designed to tackle the stability and safety challenges of PSGS during this transient process. Here, two different working modes of the closing devices, i.e., separate closing of guide vane (closing law 1) and linkage closing with guide vane and ball valve (closing law 2), are chosen from an existing PSGS in China [29-31]. The technical details of this station are listed in table 2.

Table 2: Technical details of the existing PSGS in China, adopted for safety assessment [29-31]

Parameter	**Value**
Installed capacity	4×300 MW
Nominal speed of pump-turbine	500 rpm
Water level of upstream reservoir in rejection transient	760 m
Water level of lower reservoir in rejection transient	205 m
Nominal flow of single unit	70 m^3/s

The relative opening of closing law 1 and 2 for the 30-seconds transient time is illustrated in Fig. 3. The guide vane in both closing laws adopts a linear closure mode with a constant descending movement. However, for closing law 2, the ball valve immediately initiates the system closure after the discard of load, initially closing at a higher rate. Different closing rates, shown in Fig. 2, are the result of the increasing rate in the change of hydraulic pressure.

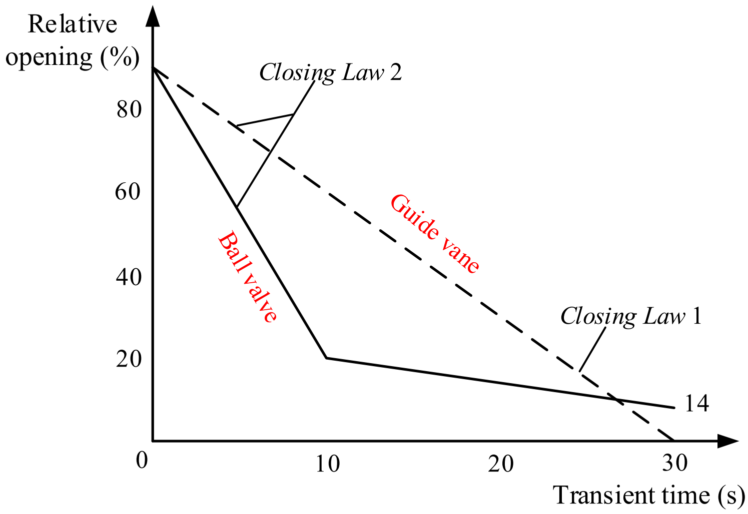

Fig. 2. Different closing laws during the 100% load rejection transient in generating mode (closing law 1 of a guide vane and closing law 2 with a guide vane and a ball valve).

Guide vane is a universal component for PSGSs, while the ball valve in closing law 2 performs the supplementary closing role for the guide vane. To illustrate the performance impact of the ball valve in an PSGS, Fig. 3 [30] provides a visual representation of the movement track of the generating system in inverted-S domain during the load rejection transient in the generating mode, i.e. varying from point 1 to point 8. It should be noted that point 4 is located in the reversed pump mode, as an adverse track point, depending on the intensity level of load rejection.

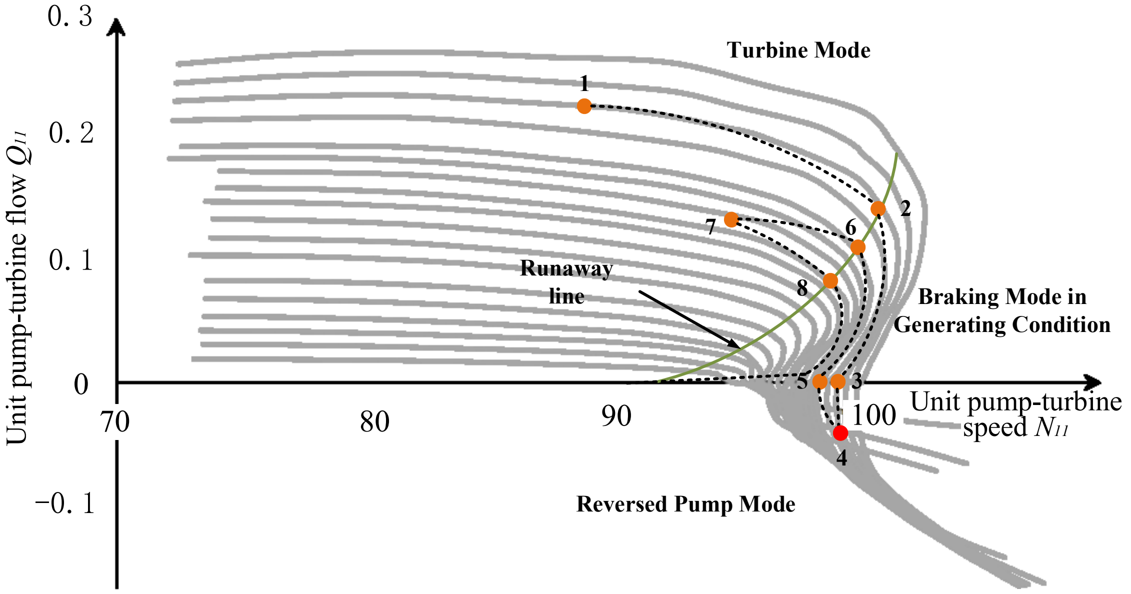

Fig. 3. Movement track of PSGS under the linkage closing law with a guide vane and a ball valve in inverted-S domain.

3. FDA method

To investigate the dynamic safety of PSGS under different closing laws of switch devices, Fisher discriminant analysis (FDA) is employed as an effective approach [32-34]. Overall, the concept of FDA is to find an optimal projection plane which would produce maximally different discrimination between training groups, where the appropriate discriminant rule is chosen to recognize the predicted samples. The working principle of FDA is shown in Fig. 4.

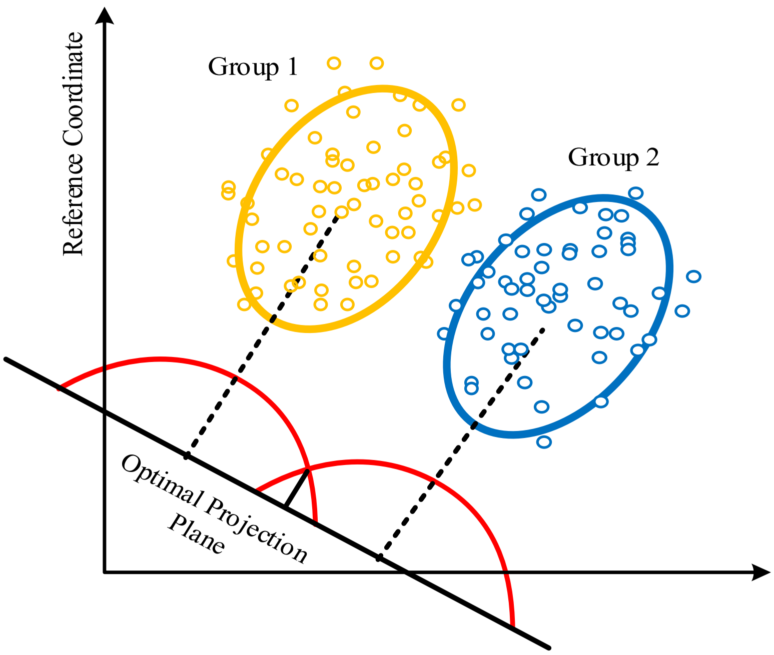

Fig. 4. Working principle of FDA.

For training groups G_i (i = $1, 2, ..., k$), their corresponding mean matrix and covariance matrix of the samples from p-dimensional space are respectively $\boldsymbol{\mu}_i$ and $\boldsymbol{\Sigma}_i$. $\boldsymbol{X}$, and $\boldsymbol{u}$ ($\boldsymbol{u} = u_1, u_2, ...$) represents the linear discriminant coefficient that directly determines the discriminant rule. When a linear discriminant function $\boldsymbol{u'X}$ is considered, its mean and variance can be estimated as:

$$\begin{cases} E\left(\boldsymbol{u'X}\right) = \boldsymbol{u'}E\left(\boldsymbol{X} \mid G_i\right) = \boldsymbol{u'\mu}_i \\ D(\boldsymbol{u'X}) = \boldsymbol{u'}D\left(\boldsymbol{X} \mid G_i\right)\boldsymbol{u} = \boldsymbol{u'\Sigma}_i\boldsymbol{u} \end{cases}, \quad i = 1, 2, \ldots, k. \tag{8}$$

Supposing that b and e are the interclass and intraclass variances, respectively, then:

$$\begin{cases} b = \sum_{i=1}^{k}(\boldsymbol{u'\mu}_i - \boldsymbol{u'\bar{\mu}})^2 \\ e = \sum_{i=1}^{k}\boldsymbol{u'\Sigma}_i\boldsymbol{u} = \boldsymbol{u'Eu} \end{cases}, \tag{9}$$

where $\bar{\boldsymbol{\mu}}=\frac{1}{k}\begin{bmatrix} u_{11} & u_{21} & \dots & u_{p1} \\ u_{12} & u_{22} & \dots & u_{p2} \\ \dots & \dots & \dots & \dots \\ u_{1k} & u_{2k} & \dots & u_{pk} \end{bmatrix}\begin{bmatrix} 1 \\ 1 \\ \dots \\ 1 \end{bmatrix}=\frac{1}{k}\boldsymbol{M1}$ and $\boldsymbol{M}=\begin{bmatrix} \boldsymbol{\mu}_1' \\ \boldsymbol{\mu}_2' \\ \dots \\ \boldsymbol{\mu}_3' \end{bmatrix}$.

Subsequently, we can deduce $\boldsymbol{M'M}=\sum_{i=1}^{k}\boldsymbol{\mu}_i\boldsymbol{\mu}_i'$ and also simplify b as $\boldsymbol{u'Bu}$. Here, $\boldsymbol{B}=\boldsymbol{M'}(\boldsymbol{I}-\frac{1}{k}\boldsymbol{J})\boldsymbol{M}$, and both $\boldsymbol{I}$ and $\boldsymbol{J}$ are unit matrices.

The objective function with regard to the linear discriminant coefficient $\boldsymbol{u}$ is therefore written as:

$$\Phi(\boldsymbol{u})=\frac{\boldsymbol{u'Bu}}{\boldsymbol{u'Eu}}. \tag{10}$$

To make $\Phi(\boldsymbol{u})$ reach to its unique maximum, there is an assumption that $\boldsymbol{u'Eu}=1$ and $\phi(\boldsymbol{u})=\boldsymbol{u'Bu}-\lambda(\boldsymbol{u'Eu}-1)$. The derivative of $\phi(\boldsymbol{u})$ can be expressed as:

$$\begin{cases} \boldsymbol{u}'\frac{\partial\phi}{\partial\boldsymbol{u}}=2\lambda(1-\boldsymbol{u'Eu})=0 \\ \boldsymbol{u}'\frac{\partial\phi}{\partial\lambda}=\boldsymbol{u}'(\boldsymbol{u'Eu}-1)=0 \end{cases}. \tag{11}$$

We obtain Eq. (12) by simplifying Eq. (11), and Eq. (12) reveals that λ is the maximum value of $\boldsymbol{u'Bu}$ and $\boldsymbol{u}$ is the eigenvector of $\boldsymbol{E}^{-1}\boldsymbol{B}$.

$$\begin{cases} \boldsymbol{u'Bu}=\lambda \\ (\boldsymbol{E}^{-1}\boldsymbol{B}-\lambda\boldsymbol{I})\boldsymbol{u}=0 \end{cases}. \tag{12}$$

Therefore, the eigenvector $\boldsymbol{u}$ = u_1, u_2, ... corresponding to the largest eigenvalue is estimated. Finally, the discriminant rule is obtained as:

$$U(\boldsymbol{X})=u_1X_1+u_2X_2+\dots+u_pX_p=\boldsymbol{u'X}. \tag{13}$$

To further explain the application of FDA in the dynamic safety assessment of PSGS, we add a diagram of global methodology shown in Fig. 5.

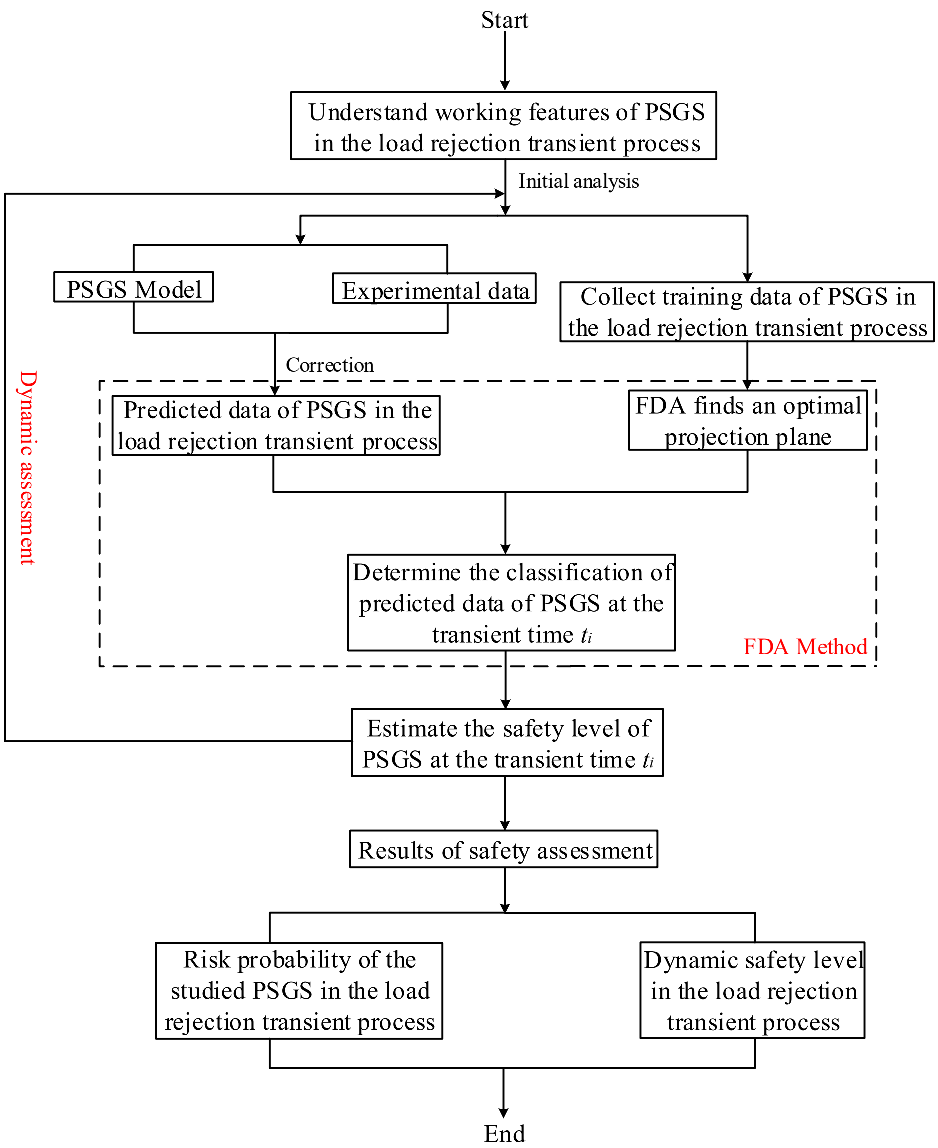

Fig. 5. Diagram of global methodology used in this paper.

4. Dynamic safety assessment of a transient PSGS

In this section, **IBM SPSS Statistics 22.0** software (SPSS) containing the algorithm of FDA is used to analyze the dynamic safety level of a nonlinear PSGS. The data used as the training groups of FDA in table 4 are extracted from several operating pump storage power units [35-37]. The operational parameters considered for the risk assessment analysis are the flow rate and speed of the pump-turbine, pressure of the draft tube and the spiral case pressure. Four levels of safety composed of Stable, Medium, Unstable and High Risk are considered for the analysis from which one is assigned to each configuration of the training group. This assignment is based on the available statistical information as well as expert judgment, since there is no unified standard available to categorize the risk of a nonlinear PSGS. The properties of the four safety levels are given in table 3. To conduct the prediction process, thirty samples of PSGS operation parameters for both transient processes under separate closing law 1 and 2 are selected based on the validated PSGS model and experimental data presented in literatures [26-31], as listed in table 5.

Table 3: Properties of the four safety levels for an PSGS

Safety levels	**Properties**
Stable	PSGS operates normally
Medium	PSGS vibrates slightly without failures
Unstable	PSGS vibrates strongly with repairable failures
High Risk	PSGS cannot able to work with irreparable failures

Table 4: Training groups of a nonlinear PSGS for rejection transient from references [35-37]

Relative Deviations for Variables of a Nonlinear PSGS (p.u.)				
Pump-turbine flow	*Pump-turbine speed*	*Pressure of draft tube*	*Pressure of spiral case*	*Safety level*
0.0033	-0.0009	0.0396	0.0024	Stable
-1.1875	0.0119	0.1897	0.004	Stable
-1.072	-0.038	0.2464	-0.0359	Stable
-0.9355	-0.0689	0.3126	-0.0783	Stable
-0.7673	-0.0608	0.3215	-0.1614	Stable
-0.6262	-0.0357	0.2665	-0.1898	Stable
-0.5208	-0.0129	0.2021	-0.0906	Stable

-0.4773	0.0262	0.0088	0.025	Stable
-1.1394	0.076	0.1607	0.3356	Stable
-1.1247	0.0138	0.0638	0.1789	Stable
-1.0891	-0.0357	0.1282	0.011	Stable
-1.0239	-0.0646	0.2234	-0.0017	Stable
-0.9588	-0.0832	0.2234	-0.0059	Stable
-0.9937	-0.0936	0.2234	-0.0034	Stable
-0.8782	-0.1141	0.2234	-0.0059	Stable
-0.4045	0.0337	0.156	0.1324	Stable
-1.1697	0.0589	0.0667	0.0024	Stable
-1.0037	-0.0571	0.0514	0.0501	Stable
-0.0168	0.146	-0.0527	0.0814	Medium
-1.2053	0.1977	-0.0479	0.2114	Medium
-1.2426	0.0903	0.0579	0.1028	Medium
-0.5409	0.0965	-0.0438	0.1266	Medium
-0.6215	0.144	-0.0556	0.1719	Medium
-0.7092	0.1668	-0.094	0.2027	Medium
-0.8301	0.1649	-0.1372	0.2213	Medium
-0.9534	0.1402	-0.0603	0.2566	Medium
-1.0867	0.1131	-0.1697	0.3356	Medium
-1.2428	0.1287	0.1377	-0.0881	Medium
-0.075	0.2352	-0.0574	0.1307	Unstable
-0.1781	0.3241	-0.1372	0.2027	Unstable
-0.8425	0.3303	-0.2063	0.3159	Unstable
-1.1224	0.2681	-0.188	0.2776	Unstable
-1.0219	0.3151	-0.1923	0.308	Unstable
-0.1297	0.3012	-0.0756	0.1665	Unstable
-0.7417	0.2476	-0.1419	0.306	Unstable
-0.3316	0.3759	-0.1892	0.2624	High Risk
-0.4928	0.3983	-0.1987	0.2933	High Risk
-0.6867	0.384	-0.2631	0.3089	High Risk
-1.0386	0.3517	-0.1632	0.4118	High Risk
-0.2451	0.362	-0.1934	0.2241	High Risk
-0.8383	0.3721	-0.3196	0.3109	High Risk
-0.4364	0.3915	-0.1893	0.2813	High Risk

Table 5: Samples of nonlinear PSGS parameters for prediction of operation safety level under closing law 1 and 2 during 100% load rejection transient process [26-31]

Predicted Samples of a Nonlinear PSGS under Different Closing Laws								
Time (s)	**Closing Law 1 (relative deviations, p.u.)**				**Closing Law 2 (relative deviations, p.u.)**			
	Pump-turbine flow	*Pump-turbine speed*	*Pressure of draft tube*	*Pressure of spiral case*	*Pump-turbine flow*	*Pump-turbine speed*	*Pressure of draft tube*	*Pressure of spiral case*
0	-0.006	-0.0028	0.0395	0.0323	-0.0038	-0.0052	0.0369	0.0247
1	-0.0294	0.1128	-0.0224	0.0703	-0.0248	0.1199	-0.0273	0.0703
2	-0.0913	0.2253	-0.0471	0.1368	-0.0816	0.2205	-0.062	0.1368
3	-0.1791	0.3115	-0.1608	0.1975	-0.1673	0.321	-0.1485	0.1956
4	-0.308	0.3727	-0.1732	0.2602	-0.3101	0.3703	-0.1683	0.2563
5	-0.4862	0.3946	-0.1856	0.2924	-0.4682	0.3969	-0.1831	0.2943
6	-0.667	0.3874	-0.2252	0.3058	-0.6678	0.3921	-0.2276	0.3076
7	-0.8607	0.3262	-0.1683	0.3152	-0.8367	0.3333	-0.1633	0.3134
8	-1.0209	0.2745	-0.193	0.2791	-1.0158	0.2721	-0.1856	0.2773
9	-1.1552	0.2106	-0.0917	0.2108	-1.1583	0.2229	-0.109	0.207
10	-1.1915	0.1493	0.069	0.0931	-1.1869	0.1394	0.069	0.0912
11	-1.176	0.0734	0.0839	0.0114	-1.1604	0.0758	0.0963	-0.0057
12	-1.1292	0.0071	0.2075	-0.0475	-1.0984	0.0218	0.2124	-0.0266
13	-0.9899	-0.0247	0.3088	-0.0892	-0.9847	-0.0275	0.3187	-0.0816
14	-0.8351	-0.0517	0.2791	-0.1671	-0.8501	-0.0518	0.2248	-0.1576
15	-0.667	-0.0565	0.341	-0.1937	-0.7256	-0.0569	0.2941	-0.1994
16	-0.5172	-0.0175	0.3088	-0.0968	-0.6015	-0.0223	0.2199	-0.1709
17	-0.4063	0.0365	0.1507	0.0247	-0.5495	0.0047	0.0765	-0.1272
18	-0.4088	0.0905	0.0296	0.1159	-0.5575	0.0389	0.0245	-0.0816
19	-0.4477	0.1493	-0.0447	0.1728	-0.5885	0.0611	0.0073	-0.0475
20	-0.5327	0.2058	-0.0842	0.2013	-0.6249	0.083	-0.0051	-0.0114
21	-0.6439	0.2304	-0.0991	0.2222	-0.674	0.1001	0.0073	0.019
22	-0.7732	0.2451	-0.146	0.2545	-0.7076	0.1175	-0.0026	0.0456
23	-0.9175	0.2304	-0.1658	0.3304	-0.7541	0.1223	0.0022	0.0703
24	-1.0493	0.2133	-0.1683	0.3304	-0.7852	0.1199	0.0073	0.0931
25	-1.1526	0.1517	0.0197	0.1709	-0.8447	0.1199	0.0172	0.1216
26	-1.176	0.0758	0.0197	-0.0038	-0.8992	0.1028	0.0172	0.1424
27	-1.1346	0.017	0.0197	-0.0133	-0.9562	0.0953	0.0172	0.152

28	-1.0544	-0.0446	0.0197	-0.0019	-1.0028	0.0707	0.0172	0.1387
29	-0.9849	-0.0764	0.0197	-0.0437	-0.9818	0.0413	0.0172	0.112
30	-0.928	-0.0764	0.0197	-0.095	-0.9327	0.0047	0.0172	0.076

Upon training the FDA model the dynamic safety levels of the nonlinear PSGS are predicted regarding closing laws 1 and 2 during 100% load rejection transient. Fig. 6 presents the estimated safety level of the generating system throughout the transition period where dynamic safety curves are plotted to better illustrate the variable characteristics and the escalation of the system risk level.

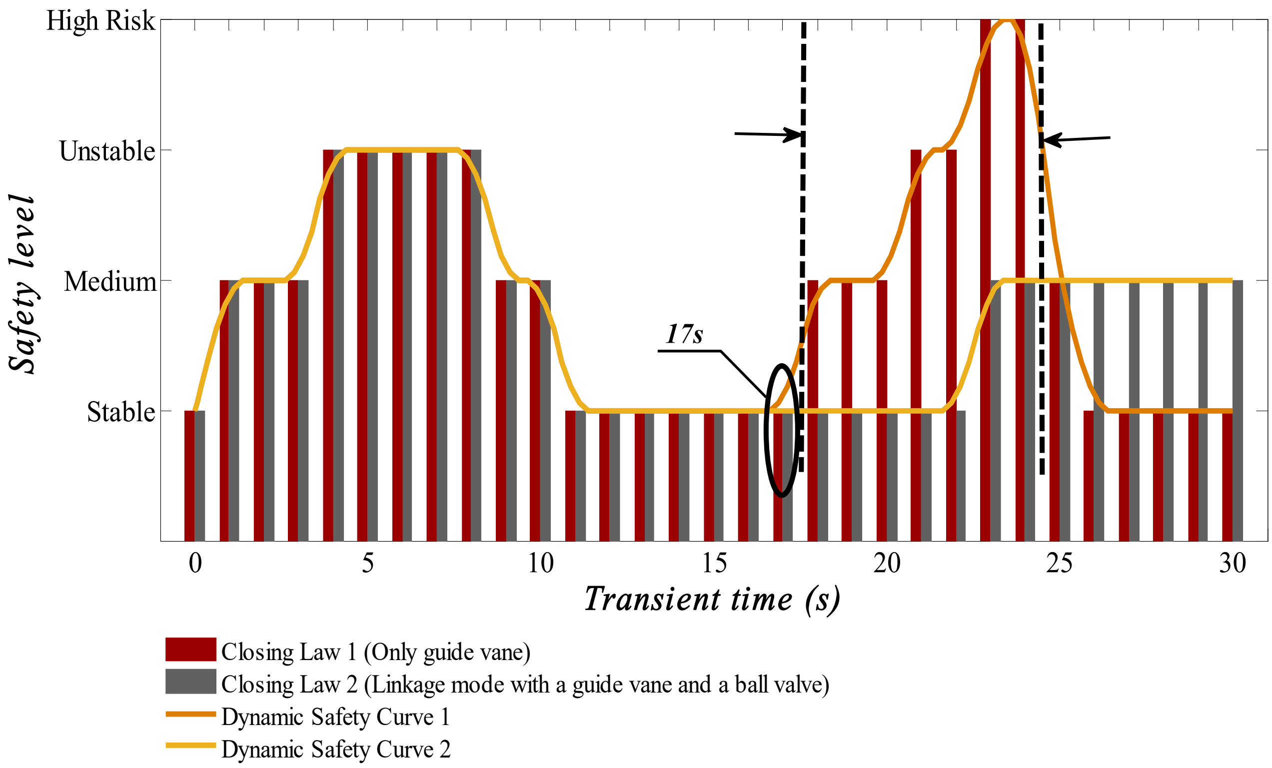

Fig. 6. Dynamic safety level of the nonlinear PSGS during 100% load rejection transient process under closing laws 1 and 2.

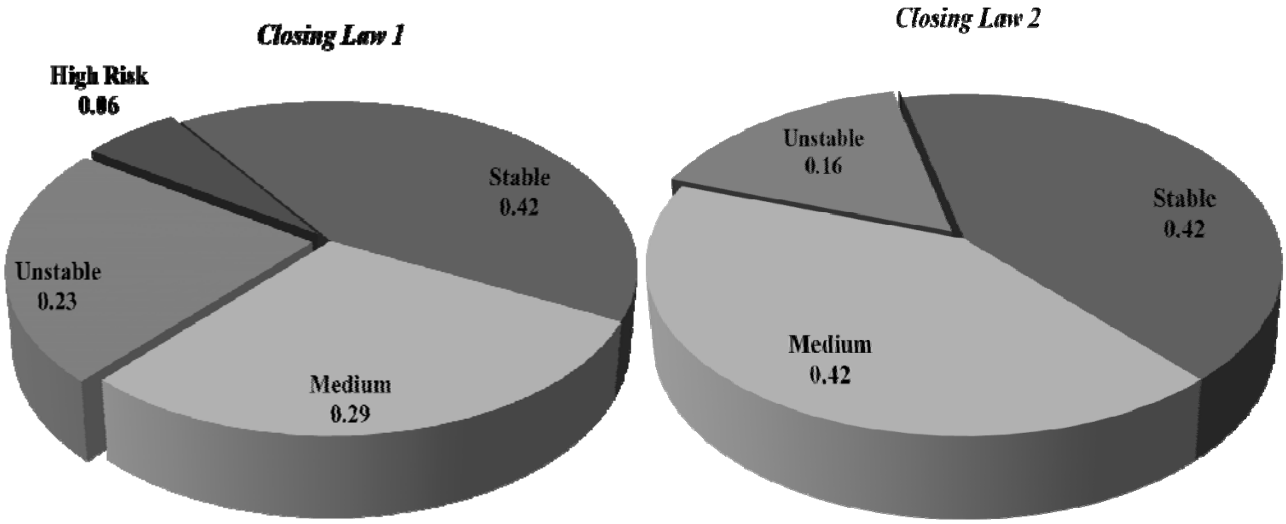

(a) (b)

Fig. 7. Comparison of estimated occurrence probability of each safety level with respect to closing law 1 and 2.

In Fig. 6, it is observed that the PSGS in load rejection operation becomes critical at time t = 17s. That is, the operation of PSGS is safe within the time interval [0, 17] because the risk level is not estimated as high for either of the assessed closing laws. The state of the generating system is predicted as unstable during the transient time t = [4, 8]. Although this cannot collapse the generating system, the vibration impact caused by the drastic change in system variables should be taken into consideration. The difference in safety levels between two closing laws appears at transient time t = 17s. In the time range t = [17, 30], the PSGS with closing law 2 controlled by the linkage mode with a guide vane and a ball valve provides a steadier operation observing only stable and medium safety levels. Conversely, the generating system with closing law 1, relying only on a guide vane closing, generates the most unfavorable condition associated with high risk during this period (as highlighted by vertical lines, the change of risk level is extremely fast within the time t = [18, 25]). These results highlight the importance of including a ball valve in the closing process of the guide vane. That is, the ball valve can play a supporting role in system stabilization. The dynamic characteristic of PSGS during the transient process is then improved significantly by adopting an appropriate closing law of switch devices.

Fig. 7 presents the estimated occurrence probability of each risk level for PSGS load rejection process. A comparison of the results between the two closing laws clearly indicates that the high risk state in closing law 1 reaches 0.06 while this probability is zero for closing law 2. Furthermore, the probability of experiencing an unstable condition is approximately 0.23, when the generating system operates in closing law 1, while this is only 0.16 for closing law 2. The probability of encountering unexpected conditions in the PSGS operation is therefore close to 0.13, suggesting that a suitable linkage closing law that uses a guide vane, as well as taking advantage of a ball valve to support the system stability, is significantly beneficial for improving the dynamic characteristics of PSGSs during closing. It is worth mentioning that the obtained results are consistent with the engineering applications in literatures [26, 30-31, 35-39].

5. Discussion

As mentioned in subsection 2.1, the predicted data of PSGS for the load rejection transient process are from the validated PSGS model and experimental data presented in literatures [26-31]. Although the study in this paper better achieves the dynamic safety assessment of PSGS in the load rejection transient process, there are still some weaknesses for predicted data of PSGS due to the precision of PSGS model. In addition to this, the training data of PSGS are also limited by the data size.

6. Conclusions

This paper presents a novel framework for safety assessment of nonlinear PSGSs, mainly focusing on answering two critical questions: a) Can the optimal closing law for a safe operation of nonlinear PSGSs be determined? and b) How can a dynamic safety analysis using FDA be carried out? For this purpose, two widely used closing laws of this system, the separate closing of a guide vane (i.e., closing law 1) and linkage closing with a guide vane and a ball valve (i.e., closing law 2), are selected from an existing pumped-storage power station. The dynamic risk level of the two closing laws is accurately estimated for a nonlinear PSGS in transient process. We find that the risk probability for closing law 1 is 0.06, while for closing law 2 it is zero. Additionally, the probability that the PSGS runs in an unstable state for closing law 1 reaches 0.23, conversely, 0.16 for closing law 2. It is also demonstrated that the obtained results are in good agreement with the corresponding theory and actual operation in hydropower stations, which can be found in literatures [26, 30-31, 35-39]. For instance, based on the result of the risk probability of PSGSs, we conclude that the PSGS controlled by the linkage closing mode would incorporate a lower overall risk level than the unit operating with only a guide vane. This is consistent with the engineering application in the literature [26]. We suggest that the proposed framework can be readily adopted to approach the dynamic risk assessment of complex engineering applications. Different dynamic processes have different properties, and the corresponding improved methods in PSGS stability are also different. Thus, future work will focus on the safety properties during other dynamic processes.

Acknowledgements

This research is supported by the scientific research foundation of the National Natural Science Foundation of China--Outstanding Youth Foundation (51622906), National Natural Science Foundation of China (51479173), Fundamental Research Funds for the Central Universities (201304030577), Scientific research funds of Northwest A&F University (2013BSJJ095), Science Fund for Excellent Young Scholars from Northwest A&F University and Shaanxi Nova program (2016KJXX-55).

References

[1] Zuo ZG, Fan HG, Liu SH, Wu YL. S-shaped characteristics on the performance curves of pump-turbines in turbine mode - A review. Renew. Sust. Energ. Rev. 2016; 60: 836-851.

[2] Perez-Diaz JI, Sarasua JI, Wilhelmi JR. Contribution of a hydraulic short-circuit pumped-storage power plant to the load-frequency regulation of an isolated power system. Int. J. Electr. Power Energy Syst. 2014; 62: 199-211.

[3] Singh NP, Singh AK, Singh AK, Agnihotri P. Effects of thermophoresis on hydromagnetic mixed convection and mass transfer flow past a vertical permeable plate with variable suction and thermal radiation. Commun. Nonlinear Sci. Numer. Simul. 2011; 16: 2519-34.

[4] Zhang LK, Ma ZY, Wu QQ, Wang XN. Vibration analysis of coupled bending-torsional rotor-bearing system for hydraulic generating set with rub-impact under electromagnetic excitation. Arch. Appl. Mech. 2016; 86: 1665-1679.

[5] Li HH, Chen DY, Zhang H, Wang FF, Ba DD. Nonlinear modeling and dynamic analysis of a hydro-turbine governing system in the process of sudden load increase transient. Mech. Syst. Signal

Proc. 2016; 80: 414-428.

[6] Anilkumar TT, Simon SP, Padhy NP. Residential electricity cost minimization model through open well-pico turbine pumped storage system. Appl. Energy 2017; 195: 23-35.

[7] Kougias I, Szabo S. Pumped hydroelectric storage utilization assessment: Forerunner of renewable energy integration or Trojan horse? Energy 2017; 140: 318-329.

[8] Xu BB, Chen DY, Zhang H, Wang FF, Zhang XG, Wu YH. Hamiltonian model and dynamic analyses for a hydro-turbine governing system with fractional item and time-lag. Commun. Nonlinear Sci. Numer. Simul. 2017; 47: 35-47.

[9] Esmaeilpour M, Domairry G, Sadoughi N, Davodi AG. Homotopy Analysis Method for the heat transfer of a non-Newtonian fluid flow in an axisymmetric channel with a porous wall. Commun Nonlinear Sci Numer Simul 2010; 15: 2424-30.

[10] Weitzel T, Glock CH. Energy management for stationary electric energy storage systems: A systematic literature review. Eur. J. Oper. Res. 2018; 246: 582-606.

[11] Mohanpurkar M, Ouroua A, Hovsapian R, Luo YS, Singh M, Muijadi E, Gevorgian V, Donalek P. Real-time co-simulation of adjustable-speed pumped storage hydro for transient stability analysis. Electr. Pow. Syst. Res. 2018; 154: 276-286.

[12] Xu BB, Wang FF, Chen DY, Zhang H. Hamiltonian modeling of multi-hydro-turbine governing systems with sharing common penstock and dynamic analyses under shock load. Energ. Convers. Manage. 2016; 108: 478-487.

[13] Li DY, Gong RZ, Wang HJ, Wei XZ, Liu ZS, Qin DQ. Numerical investigation on transient flow of a high head low specific speed pump-turbine in pump mode. J. Renew. Sustain. Ener. 2015; 7.

[14] Li B, Duan ZT, Wang X, Wu JZ. Loss-of-excitation analysis and protection for pumped-storage machines during starting. IET Renew. Power Gen. 2016; 10: 71-78.

[15] Mason DP, Hill DL. Invariant solution for an axisymmetric turbulent free jet using a conserved vector. Commun. Nonlinear Sci. Numer. Simul. 2013; 18: 1607-1622.

[16] Schmidt J, Kemmetmuller W, Kugi A. Modeling and static optimization of a variable speed pumped storage power plant. Renew. Energy 2017; 111: 38-51.

[17] Mennemann JF, Schmidt J, Kemmetmuller W, Kugi A. Simulation of wave effects in pumped-storage power plants using the spectral element method. AT-Autom. 2016; 64: 681-695.

[18] Vereide K, Svingen B, Nielsen TK, Lia L. The effect of surge tank throttling on governor stability, power control, and hydraulic transients in hydropower plants. IEEE Trans. Energy Convers. 2017; 32: 91-98.

[19] Vereide K, Lia L, Nielsen TK. Hydraulic scale modelling and thermodynamics of mass oscillations in closed surge tanks. J. Hydraul. Res. 2015; 53: 519-524.

[20] Li DY, Wang HJ, Qin YL, Wei XZ, Qin DQ. Numerical simulation of hysteresis characteristic in the hump region of a pump-turbine model. Renew. Energ. 2018; 115: 433-447.

[21] Patelli E, Govers Y, Broggi M, Gomes HM, Link M, Mottershead JE. Sensitivity or Bayesian model updating: a comparison of techniques using the DLR AIRMOD test data. Arch. Appl. Mech. 2017; 87: 905-925.

[22] Au SK, Patelli E. Rare event simulation in finite-infinite dimensional space. Reliab. Eng. Syst. Saf. 2016; 148; 67-77.

[23] Munir A. Safety Assessment and Design of Dependable Cybercars For today and the future. IEEE

Consum. Electron. Mag. 2017; 6: 69-77.

[24] Ding XW, Chong X, Bao ZF, Xue Y, Zhang SH. Fuzzy Comprehensive Assessment Method Based on the Entropy Weight Method and Its Application in the Water Environmental Safety Evaluation of the Heshangshan Drinking Water Source Area, Three Gorges Reservoir Area, China. Water 2017; 9.

[25] Wrobel K, Montewka J, Kujala P. Towards the assessment of potential impact of unmanned vessels on maritime transportation safety. Reliab. Eng. Syst. Saf. 2017; 165: 155-169.

[26] Yang JD, Yang JB. Checking calculation and analysis on transient process of Huizhou pumped storage power plant in commissioning period. 1st ed. Wuhan: Wuhan University; 2010 [in Chinese].

[27] Yang JD, Zeng W, Yang WJ, Yao SW, Guo WC. Runaway stabilities of pump-turbines and its correlations with S characteristic curves. Transactions of the Chinese Society for Agricultural Machinery 2015; 4 [in Chinese]. Doi: 10.6041/j.issn.1000-1298.2015.04.010

[28] Zhang XX, Cheng YG, Xia LS, Yang JD, Qian ZD. Looping Dynamic Characteristics of a Pump-Turbine in the S-shaped Region During Runaway. J. Fluid Eng.-T. ASME 2016; 138.

[29] Hou CS, Cheng YG. Optimized closing procedures of wicket gate and ball valve for high head reversible pump-turbine unit. Journal of Wuhan University of Hydraulic and Electric Engineering 2005; 38 [in Chinese].

[30] Zhang C, Yang JD. Study on linkage closing rule between ball valve and guide vane in high head pumped storage power station. Water Resources and Power 2011; 29 [in Chinese].

[31] Zhang C. Study on transition process of load successive rejection of multiple units per penstock in pumped storage hydropower power station. Water Resources and Hydropower Engineering 2011; 42 [in Chinese]. Doi: 10.13928/j.cnki.wrahe.2011.12.019

[32] Li XW, Jiang CL, Tang J, Chen YJ, Yang DD, Chen ZX. A Fisher's Criterion-Based Linear Discriminant Analysis for Predicting the Critical Values of Coal and Gas Outbursts Using the Initial Gas Flow in a Borehole. Math. Probl. Eng. 2017.

[33] Van M, Kang HJ. Bearing Defect Classification Based on Individual Wavelet Local Fisher Discriminant Analysis with Particle Swarm Optimization. IEEE Trans. Ind. Inform. 2016; 12: 124-135.

[34] Filisbino TA, Giraldi GA, Thomaz C. Ranking Tensor Subspaces in Weighted Multilinear Principal Component Analysis. Int. J. Pattern Recognit. Artif. Intell. 2017; 31.

[35] Wei SP. Simulation of hydraulic turbine regulating system. 1st ed. Wuhan: Huazhong University of Science and Technology Press; 2011 [in Chinese]. ISBN: 978-7-5609-7148-3

[36] Li JH, Zhu HF. Optimization on closing law of globe valve and guide blade after load rejection in Huizhou pumped storage units. Guangdong Electric Power 2012; 25 [in Chinese].

[37] Lin K. Measured results and simulation analysis of transient process of pumped storage unit in Huizhou. Guangdong Electric Power 2011; 24 [in Chinese].

[38] Chang JS. Transients of hydraulic machine installations. 1st ed. Beijing: China Higher Education Press; 2005 [in Chinese]. ISBN: 7-04-017647-5

[39] Cui BL, Lin Z, Zhu ZC, Wang HJ, Ma GF. Influence of opening and closing process of ball valve on external performance and internal flow characteristics. Exp. Therm. Fluid Sci. 2017; 80: 193-202.